Human Molecular Genetics, 2012, Vol. 21, No. 11 **2485–2496**
doi:10.1093/hmg/dds063
Advance Access published on February 24, 2012

Tbx1 is a negative modulator of *Mef2c*

Luna Simona Pane[1,2], Zhen Zhang[3], Rosa Ferrentino[1,2], Tuong Huynh[4], Luisa Cutillo[2,5] and Antonio Baldini[1,2,6,*]

[1]Institute of Genetics and Biophysics, National Research Council, 80131 Naples, Italy, [2]Telethon Institute of Genetics and Medicine, 80131 Naples, Italy, [3]Shanghai Pediatric Congenital Heart Disease Institute, Shanghai Children's Medical Center, Shanghai Jiao Tong University School of Medicine, Shanghai 200092, China, [4]Baylor College of Medicine, Houston, TX 77030, USA, [5]University of Naples Parthenope, 80133 Naples, Italy and [6]University of Naples Federico II, 80143 Naples, Italy

Received December 8, 2011; Revised and Accepted February 20, 2012

The developmental role of the T-box transcription factor Tbx1 is exquisitely dosage-sensitive. In this study, we performed a microarray-based transcriptome analysis of E9.5 embryo tissues across a previously generated *Tbx1* mouse allelic series. This analysis identified several genes whose expression was affected by *Tbx1* dosage. Interestingly, we found that the expression of the gene encoding the cardiogenic transcription factor Mef2c was negatively correlated to *Tbx1* dosage. *In vivo* data revealed *Mef2c* up-regulation in the second heart field (SHF) of *Tbx1* null mutant embryos compared with wild-type littermates at E9.5. Conversely, *Mef2c* expression was decreased in the SHF and in somites of *Tbx1* gain-of-function mutants. These results are consistent with the described role of Tbx1 in suppressing cardiac progenitor cell differentiation and indicate also a negative effect of Tbx1 on *Mef2c* during skeletal muscle differentiation. We show that Tbx1 occupies conserved regulatory regions of the *Mef2c* locus, suggesting a direct effect on *Mef2c* transcription. However, we also show that Tbx1 interferes with the Gata4→ Mef2c regulatory pathway. Overall, our study uncovered a target of Tbx1 with critical developmental roles, so highlighting the power of the dosage gradient approach that we used.

INTRODUCTION

The T-box transcription factor TBX1 is encoded by the main gene haploinsufficient in DiGeorge syndrome, which is characterized by congenital heart defects, hypo/aplasia of the parathyroid and thymus glands, craniofacial dysmorphism as well as learning and behavioral abnormalities (1–5). Mutation of murine *Tbx1* can model the DiGeorge syndrome phenotype (6–8). A progressive dosage reduction in *Tbx1* mRNA is associated with the non-linear increase in phenotypic severity (9) while over-expression of *Tbx1* results in structural heart and thymic defects (10), confirming that Tbx1 function, during embryonic development, is exquisitely dosage-sensitive. Uncovering the genetic and phenotypic changes resulting from *Tbx1* haploinsufficiency might help dissection of molecular mechanisms underlying the DiGeorge syndrome etiology.

Loss of *Tbx1* is associated with reduced proliferation and premature differentiation in the second heart field (SHF) (11–14). Accordingly, *Fgf8* and *Fgf10* were down-regulated in $Tbx1^{-/-}$ mutants (13,15,16) while genes required for myocardial differentiation (like *Raldh2*, *Gata4* and *Tbx5*) were ectopically expressed (13).

The mechanisms by which Tbx1 regulates its targets are not all clear; there are now examples of transcription-dependent and transcription-independent actions. For example, *in vitro* and *in vivo* evidences show that Tbx1 positively regulates expression of the *Vegfr3* gene through interaction with a T-box-binding element (TBE) (17), as expected for T-box transcription factors.

On the other hand, it is also clear that Tbx1 can function in a transcription-independent manner. Indeed, Tbx1 is able to negatively regulate the bone morphogenic protein–Smad1 pathway by binding Smad1 and thus preventing the Smad1–

*To whom correspondence should be addressed at: Institute of Genetics and Biophysics A. Buzzati Traverso CNR, Via Pietro Castellino, 111, 80131 Napoli, Italy. Tel: +39 0816132219; Fax: +39 0816132706; Email: antonio.baldini@igb.cnr.it

Smad4 interaction (18), which is required for the activation of Smad1 target genes (19).

Furthermore, Tbx1 can interact with the serum response factor (Srf) and promote its proteasome-mediated degradation (17), which, in turn, results in cardiac actin and α-smooth muscle actin protein down-regulation (17,20,21). This non-transcriptional interaction, although not yet completely clarified, probably contributes to the inhibition of cardiomyocyte differentiation observed *in vivo* (13,14).

In this study, starting from microarray-based gene expression data, collected across an allelic series of *Tbx1* embryo mutants, we found that Tbx1 negatively modulates *Mef2c* through several mechanisms.

Mef2c belongs to the MEF2 (myocyte-specific enhancer-binding factor 2) subfamily of MADS [MCM1 (Minichromosome Maintenance 1 Protein), AG (Agamous), DEFA (Deficiens) and SRF (Serum Response Factor)] transcription factors (22). *Mef2* genes are expressed in cardiac, smooth and skeletal muscle cells, endothelial cells as well as in a restricted set of other tissues (23–25). Targeted inactivation of the *Mef2c* gene in the mouse resulted in cardiac and vascular defects and embryonic lethality at E9.5 (26–28). In particular, in $Mef2c^{-/-}$ mice, the heart tube does not undergo looping morphogenesis, the future right ventricle does not form and several cardiac muscle genes are down-regulated. These data indicate a key role of Mef2c in the transcriptional pathways controlling myocyte differentiation.

We provide *in vivo* and *in vitro* data, indicating that Tbx1 plays an inhibitory role onto the Gata4→Mef2c regulatory pathway, and we propose that this is a mechanism by which Tbx1 affects muscle cell differentiation.

Our data also highlight the power of multiallelic gene expression analysis as a tool to identify developmentally critical genes that correlate genotype-dependent phenotypic changes to genome-wide transcriptional features.

RESULTS

Identification of *Tbx1* dosage-sensitive transcripts

We have previously generated a series of genotypes associated with a nearly continuous variation of *Tbx1* mRNA dosage between 0 and 100% of the wild-type (wt) level by combining two different hypomorphic alleles, $Tbx1^{Neo2}$ and $Tbx1^{Neo}$, and a null allele, $Tbx1^{-}$ (9). To identify *Tbx1* dosage-dependent genes *in vivo*, we performed a microarray-based transcriptome analysis across the allelic series; RNA isolated from whole E9.5 embryos with nine different genotypes (9) was hybridized to Affymetrix GeneChip Mouse Genome 430 2.0 arrays. For each genotype, we used two embryos, each hybridized to one array; thus, we analyzed a total of 18 arrays (the whole set of results has been deposited in NCBI's Gene Expression Omnibus and is accessible through GEO Series accession number GSE33064; http://www.ncbi.nlm.nih.gov/geo/query/acc.cgi?token=rxiphqgaeyioipy&acc=GSE33064).

We developed a data analysis strategy to identify genes that respond significantly to dosage variation of *Tbx1* mRNA (see Materials and Methods) and we found 2230 transcripts with significant differential expression (Supplementary Material, Table S1). At a second filtering step (see Materials and Methods), we narrowed down the list to 497 transcripts (in addition to *Tbx1*) differentially expressed across the allelic series (Supplementary Material, Table S2). Among these genes, we found very limited overlaps with previously reported gene lists derived from *Tbx1* mutants (13,29); these genes are highlighted in green color in Supplementary Material, Table S2. However, those studies were carried out using different developmental stages and different experimental approaches that did not use allelic series.

We applied a Gene Ontology (GO) search to the more stringent data set using DAVID (30,31) and found 14 GO categories that are significantly enriched (Supplementary Material, Table S3).

We also carried out a cluster analysis that returned four main clusters (Fig. 1). Cluster 2 includes *Tbx1* and transcripts that have an expression trend similar to *Tbx1* across genotypes. Cluster 3 behaves in an opposite way as transcripts in this group tend to be more expressed as *Tbx1* expression goes down. Clusters 1 and 4, which are also the richest in transcripts (see Supplementary Material, Table S4, for transcript content of clusters), are very different and have somewhat complementary patterns. In these two clusters, there appears to be a threshold-like effect at dosages between experimental points 4 and 5, corresponding to genotypes $Tbx1^{+/-}$ and $Tbx1^{Neo2/Neo2}$, which are associated with a small overall difference in *Tbx1* RNA dosage (10–15%) (9), but genetically, they have an important difference, i.e. the former has an intact wt allele and the latter has none. How this genetic difference can translate into the expression patterns represented in Clusters 1 and 4 remains to be investigated.

Tbx1 negatively regulates *Mef2c* expression

Among the 497 differentially expressed genes, we noted that *Mef2c* expression increased as *Tbx1* dosage decreased (similarly to Cluster 3 of Fig. 1; Supplementary Material, Table S2). *Mef2c* is important for heart development and cardiomyocyte differentiation. The heart of *Mef2c* homozygous mutant mice does not undergo looping and has gross abnormalities in the outflow tract, while the right ventricle fails to form (28), suggesting a key role for *Mef2c* in SHF development. In particular, it regulates transcriptional pathways controlling differentiation. So, the negative modulation of *Mef2c* expression by Tbx1 could contribute to explain the role of *Tbx1* in suppressing cell differentiation (14).

We confirmed *Mef2c* up-regulation in $Tbx1^{-/-}$ embryos by quantitative real-time reverse transcriptase–polymerase chain reaction (qRT–PCR) of mRNA from E9.5 whole embryos (Fig. 2A). In addition, *in situ* hybridization (ISH) on embryo cryosections at E9.5 revealed up-regulation and ectopic expression of *Mef2c* in the SHF of $Tbx1^{-/-}$ mutants (Fig. 2F–I) compared with wt littermates (Fig. 2B–E). If *Mef2c* expression is *Tbx1* dosage-dependent *in vivo*, we expected to observe a *Mef2c* down-regulation in *Tbx1* gain-of-function mutants. Whole-mount ISH was performed on COET;$Mesp1^{Cre/+}$ embryos at E9.5; the COET (for Conditional Over-Expression of Tbx1) transgene expresses *Tbx1* mRNA in response to Cre recombination (10). $Mesp1^{Cre}$ drives *Tbx1* expression in mesodermal domains of the pharynx, head mesenchyme and splanchnic mesoderm

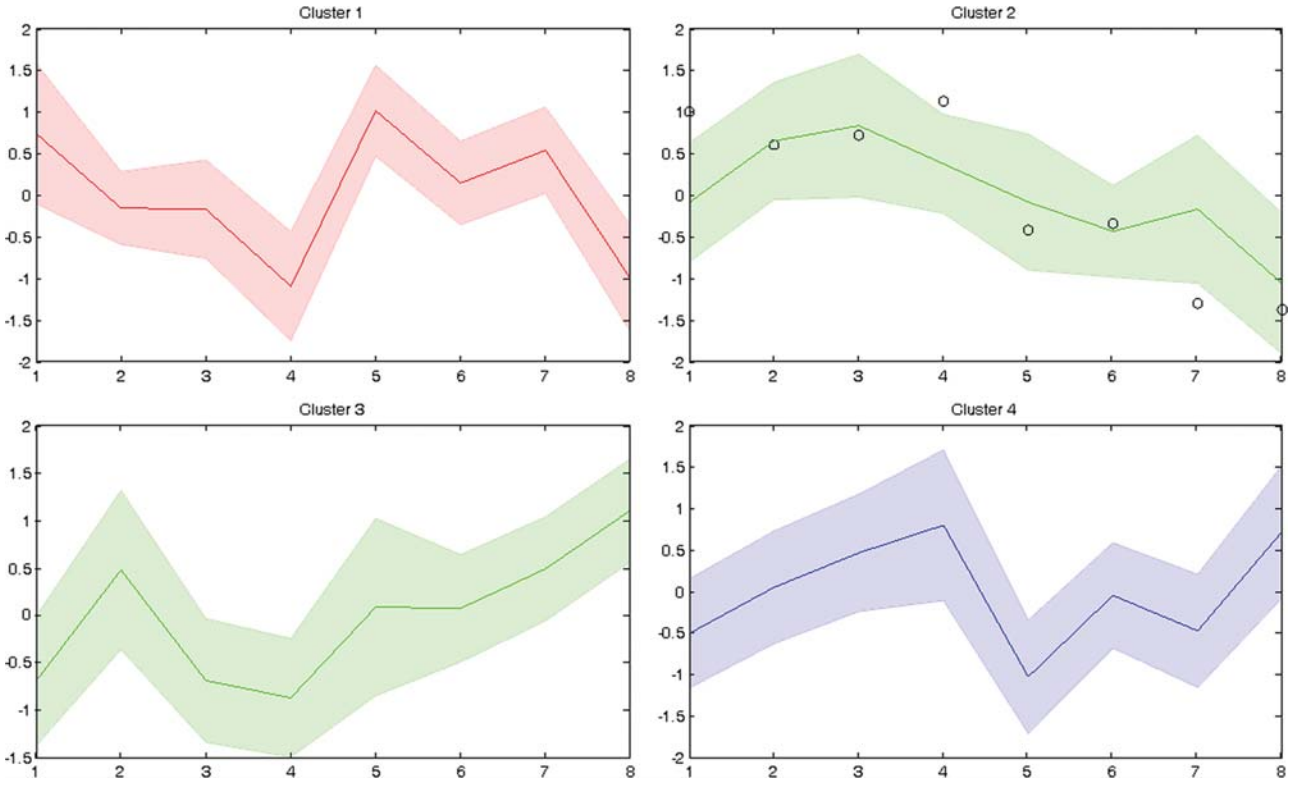

Figure 1. Cluster analysis of differentially expressed genes across the allelic series. Lines represent the average profile of each cluster and the shaded areas represent the error (SD). Profiles were obtained by plotting the log ratios of all dosage points with respect to the control (wt) point for all genes, and then, the average profile, for each cluster, was determined. *Tbx1* profile in Cluster 2 is highlighted by black circles. The transcript content of each cluster is listed on Supplementary Material, Table S4.

(Fig. 3A–D). Whole-mount ISH showed a strong reduction in *Mef2c* somite expression in COET;*Mesp1*$^{Cre/+}$ embryos (arrowheads in Fig. 3E and H) and a mild *Mef2c* down-regulation in the SHF (ovals in Fig. 3G and L) or splanchnic mesoderm (arrows in Fig. 3E, H, F and I). This different effect upon *Mef2c* expression in different tissues may be due to biological reasons (different mechanisms of regulation in different tissues) or to technical reasons (e.g. different levels of expression of the COET transgene or different efficiency of Cre-mediated excision). We confirmed that *Mef2c* expression is *Tbx1* dosage-dependent using qRT–PCR of mRNA from C2C12 myoblasts transfected with different amounts of a *Tbx1*-expressing vector (pCDNA-Tbx1-c-myc) (Fig. 4A and B). Western blotting (WB) analysis of nuclear protein extracts from transfected C2C12 cells with an anti-Mef2c antibody confirmed negative regulation at a protein level, too (Fig. 4C).

Tbx1 interferes with *Mef2c* expression and muscle cell differentiation

We tested the response of *Mef2c* expression to *Tbx1* dosage during skeletal muscle differentiation. C2C12 myoblasts can be induced to differentiate, *in vitro*, by switching culture conditions from a medium supplemented with 10% fetal bovine serum to a medium supplemented with 2% horse serum (32). Under these conditions, we observed an increased expression of myogenic markers *MyoD* and *myogenin* at day 2 of differentiation (data not shown). Also *Mef2c* expression was increased at day 2 and, interestingly, transfected *Tbx1* inhibited this up-regulation (Fig. 4D). These data are consistent with those obtained *in vivo* with the gain-of-function model (Fig. 3E–L) and suggest that Tbx1 may inhibit skeletal muscle differentiation through *Mef2c* down-regulation. To further support this hypothesis, we transfected C2C12 cells with *Tbx1*, let them differentiate for 5 days and test different skeletal muscle differentiation markers by qRT–PCR. Results showed that while *Myogenin* did not change in response to *Tbx1* transfection, all the genes encoding muscle structural proteins tested (*Myh1*, *2*, *8* and *Acta1*) were significantly down-regulated (Supplementary Material, Fig. S1). However, myotube formation did not appear to be grossly affected (data not shown).

Tbx1 inhibits Gata4- but not Isl1-induced up-regulation of Mef2c activity

To test the effects of Tbx1 upon Mef2c transcriptional activity, we performed luciferase assays using a MEF2 luciferase reporter construct (*des*MEF2-luc) on transfected C2C12 cells (33,34). With this reporter, luciferase activity is proportional to active MEF2 transcription factors. *Mef2b* is expressed at a very low level in these cells (data not shown); *Mef2a* and *Mef2d* are

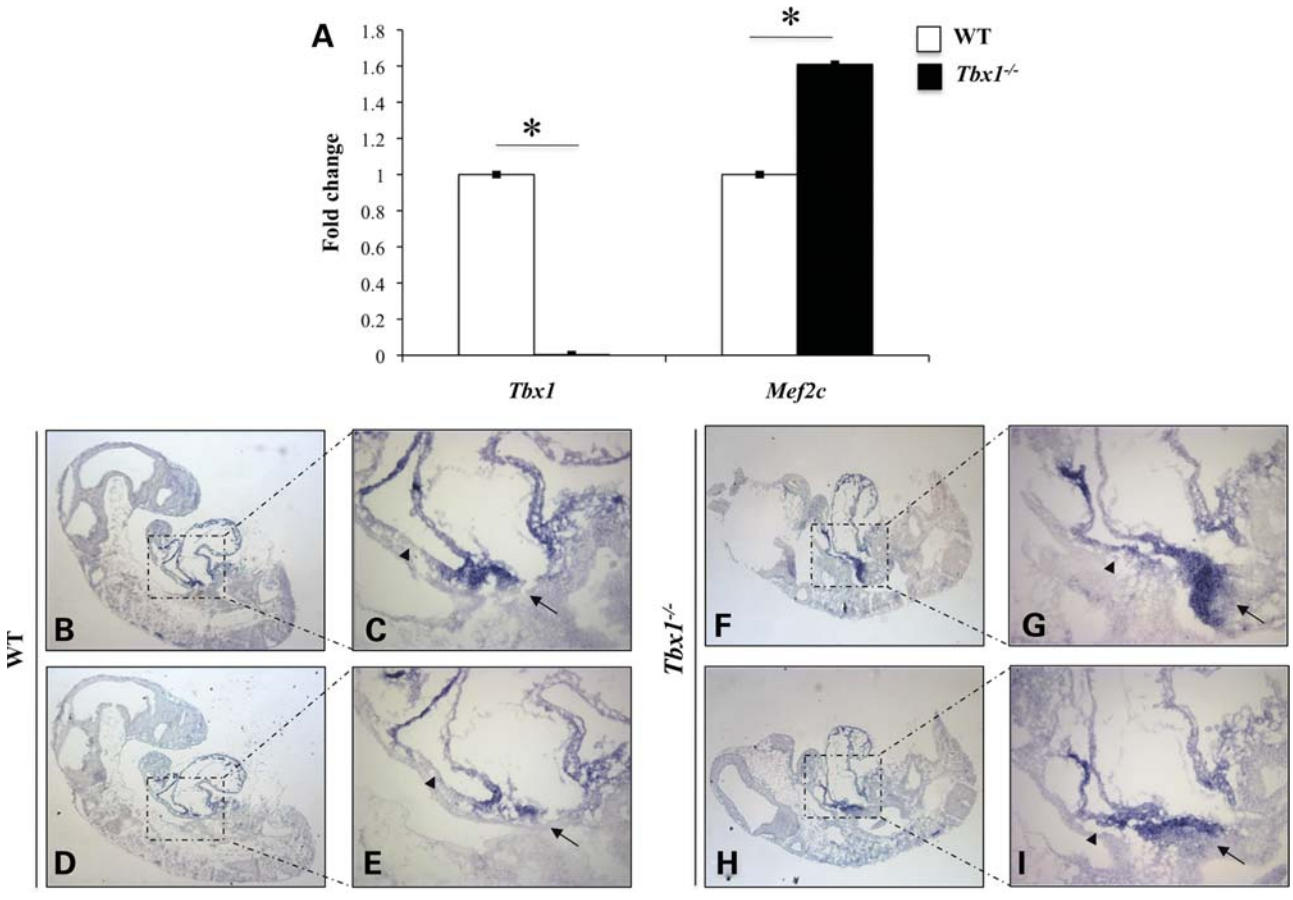

Figure 2. *Mef2c* is up-regulated in *Tbx1* loss-of-function mutants. (**A**) qRT–PCR analysis showed *Mef2c* up-regulation in *Tbx1*-null mutant embryos compared with wt littermates at E9.5. Values are means ± standard error (SE), $n = 3$, $^{*}P < 0.05$. (**B**–**I**) *Mef2c* is up-regulated (arrows) and ectopically expressed (arrowheads) in the SHF of $Tbx1^{-/-}$ mutants (G and I) compared with wt littermates at E9.5 (C and E), as shown by section ISH. (C and E) and (G and I) are high-magnification views of the same wt (B and D) and mutant sections (F and H) respectively.

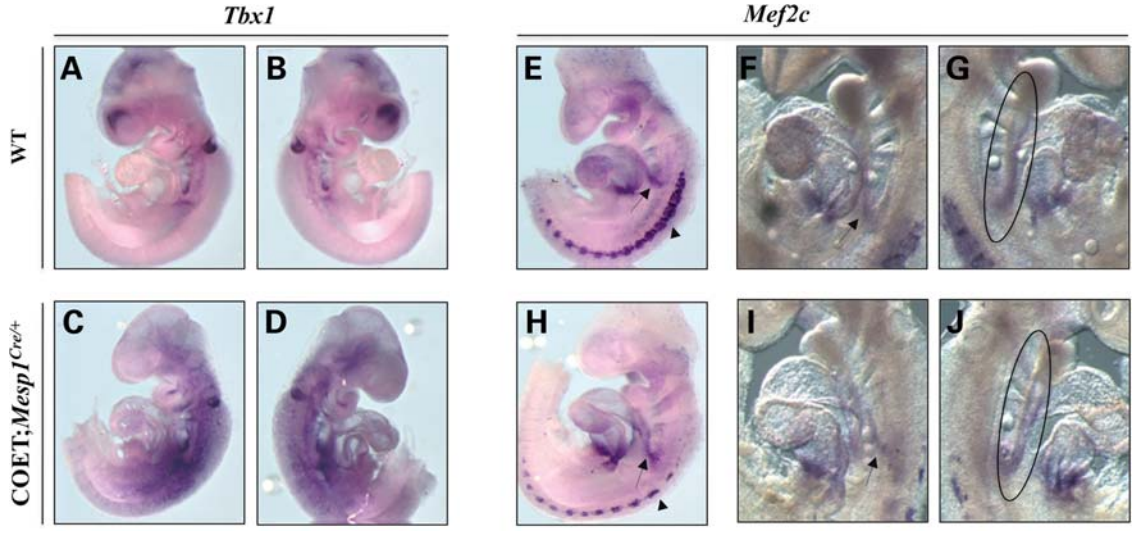

Figure 3. *Mef2c* is down-regulated in *Tbx1* gain-of-function mutants. (**A**–**L**) Left- and right-side views of whole wt (A, B and E–G) and COET; $Mesp1^{Cre/+}$ mutants (C, D, H, I and L) at E9.5. *Tbx1* is over-expressed in the mesodermal domains of the pharynx, head mesenchyme and splanchnic mesoderm of COET; $Mesp1^{Cre/+}$ mutants (C and D) compared with wt littermates (A and B). *Mef2c* is mildly down-regulated in the SHF (ovals in G and L) and splanchnic mesoderm (arrows in E, F, H and I), and more extensively in the somites (arrowheads in E and H) of COET; $Mesp1^{Cre/+}$ mutants (H, I and L) compared with wt littermates (E, F and G).

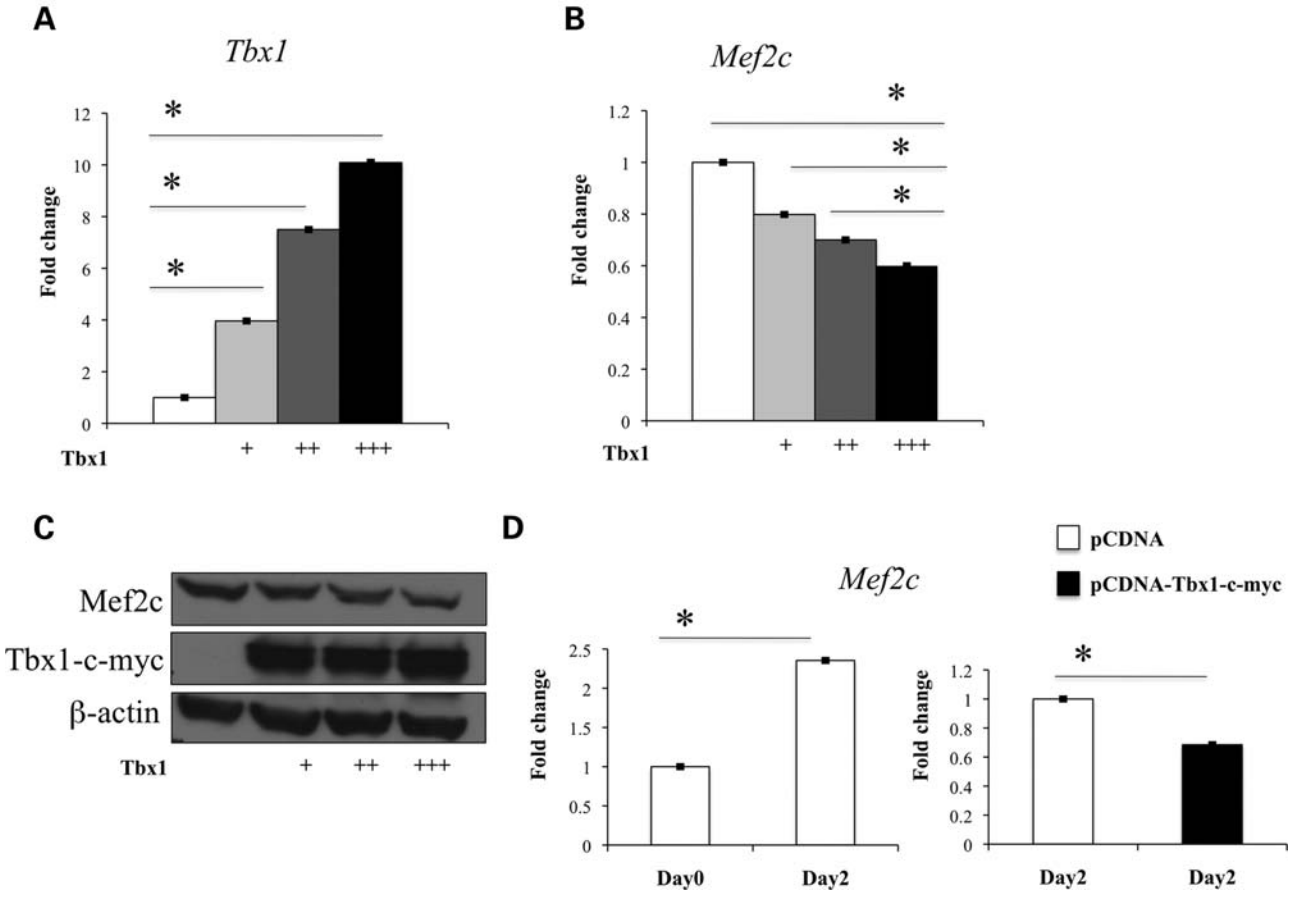

Figure 4. *Tbx1* negatively regulates *Mef2c* expression in C2C12 myoblasts. (**A**–**C**) *Mef2c* mRNA and Mef2c protein levels are affected by Tbx1 dosage in transfected C2C12 myoblasts as confirmed by qRT–PCR (A and B) and WB analysis (C). (**D**) qRT–PCR analysis showed Tbx1-dependent inhibition of *Mef2c* up-regulation during *in vitro* C2C12 myoblast differentiation. Values are means ± SE, $n = 3$, $^{*}P < 0.05$.

detectable, but their expression is not significantly affected by Tbx1 over-expression (Supplementary Material, Fig. S2). Luciferase activity increased in response to *Gata4* or *Isl1* transfection of C2C12 cells, confirming the ability of Gata4 and Isl1 to activate *Mef2c* transcription (35) also in this system (Fig. 5A and B). Transfection of a *Tbx1* expression vector alone did not affect luciferase activity (Fig. 5A). However, co-transfection of *Tbx1* and *Gata4* showed that Tbx1 inhibited the ability of Gata4 to transactivate the reporter (Fig. 5C). In contrast, Tbx1 did not inhibit the Isl1-induced activation of the reporter (Fig. 5D), suggesting that Tbx1 may regulate *Mef2c* expression through a Gata4-dependent mechanism.

It has been shown that *Gata4* is up-regulated in *Tbx1*$^{-/-}$ mutants (13). We analyzed *Gata4* expression at E8.5 and E9.5 by whole-mount ISH on control and COET;*Mesp1*$^{Cre/+}$ mutant embryos, and we found a marked *Gata4* down-regulation in COET;*Mesp1*$^{Cre/+}$ mutant hearts (Fig. 6C and D) compared with control embryos (Fig. 6A and B), thus confirming that Tbx1 can negatively affect *Gata4* expression. Since *Mef2c* is regulated by Gata4 (13), one can argue that reduced *Mef2c* expression observed in our experiments is merely the result of *Gata4* down-regulation by Tbx1. However, this is unlikely since we performed our luciferase assays on cells transfected with a *Gata4* expression vector, which is not regulated by Tbx1. Indeed, co-transfection of *Tbx1* did not affect the amount of protein produced by the *Gata4* expression vector (Supplementary Material, Fig. S3).

Gata4 is required for Tbx1-induced regulation of *Mef2c* in C2C12 cells

The previous experiments support the existence of a Tbx1-|Gata4→Mef2c pathway, but this is not sufficient to explain all our data. To test whether Tbx1 regulates *Mef2c* transcription through a mechanism involving Gata4, we evaluated the response of *Mef2c* to Tbx1 in the absence of *Gata4*. C2C12 myoblasts express endogenous *Gata4*, so, using *Gata4*-specific siRNAs, we knocked down the mRNA and protein levels to ∼20% of the wt level (Fig. 7A and B). *Gata4* knockdown was associated with down-regulation of *Mef2c* to ∼80% of the wt level (Fig. 7C). Transfection of *Tbx1* (Fig. 7D) did not result in further significant reduction in *Mef2c* expression (Fig. 7C), suggesting that Gata4 is required for Tbx1-induced down-regulation of *Mef2c*.

Tbx1 occupies conserved regions of the *Mef2c* gene

We performed a bioinformatic analysis to look for potential TBEs evolutionary conserved between the human and the mouse, in the *Mef2c* locus (see Materials and Methods). One

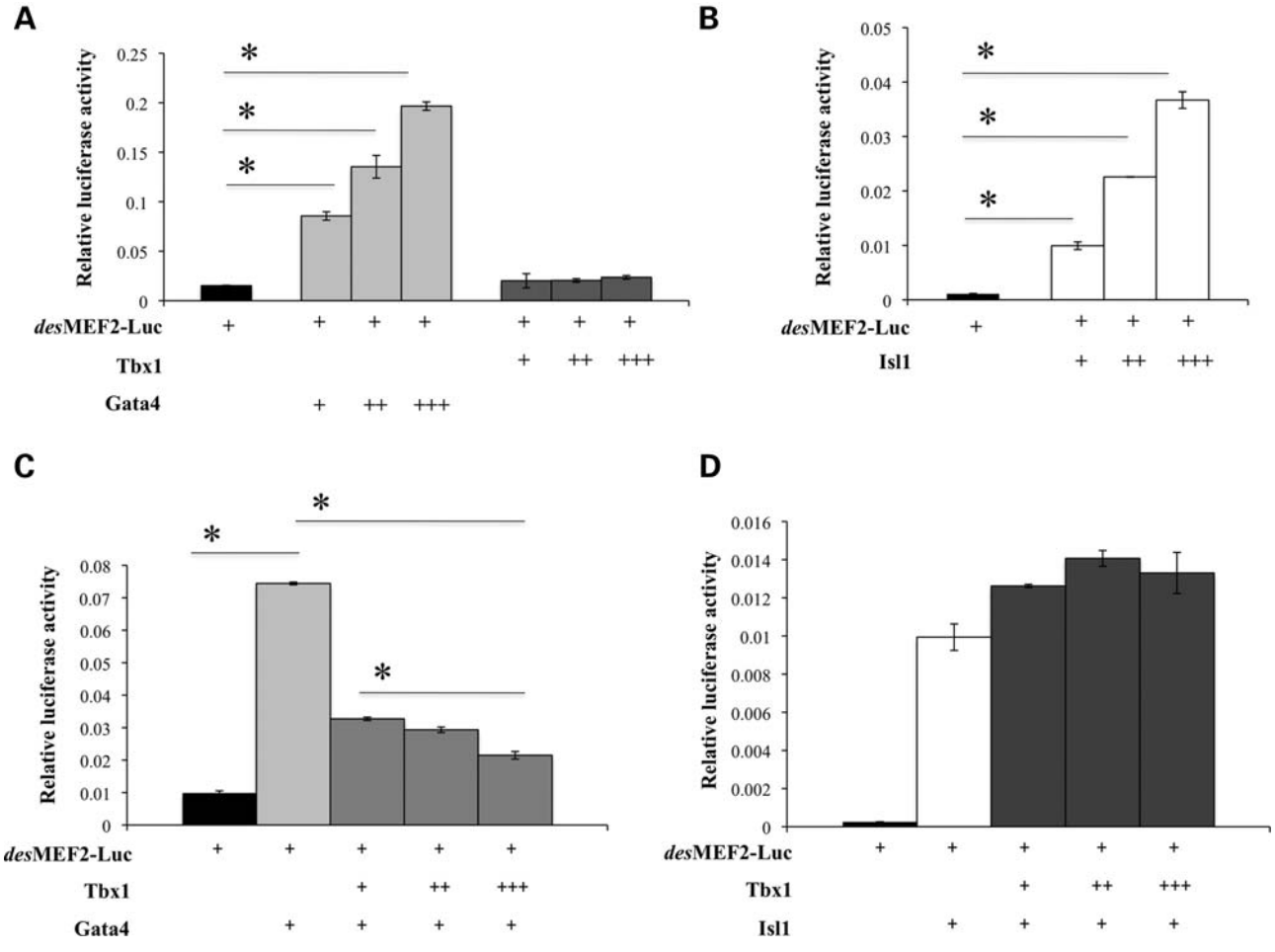

Figure 5. Tbx1 inhibits Gata4-dependent activation of the MEF2 reporter construct in luciferase assays. (**A** and **B**) Gata4 and Isl1 are able to activate the MEF2 reporter construct in transfected C2C12 cells (A and B) while Tbx1 is not able to repress it (A). (**C** and **D**) Tbx1 is able to contrasts Gata4- (C) but not Isl1-dependent activation of the MEF2 reporter construct (D). Luciferase activity was normalized to β-galactosidase activity. Values are means ± SE, $n = 3$, $^{*}P < 0.05$.

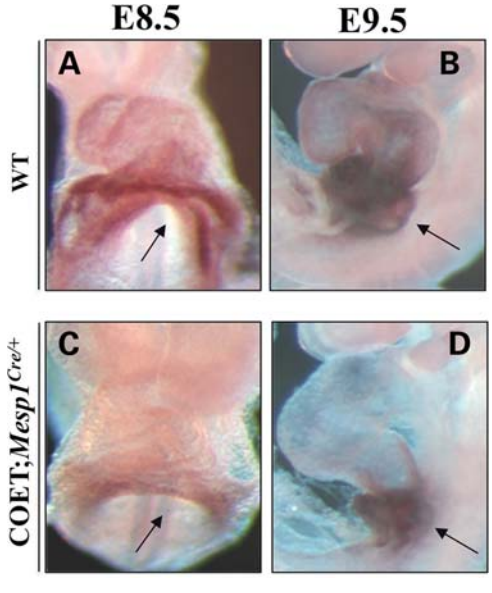

Figure 6. *Tbx1* affects *Gata4* expression *in vivo*. (**A**–**D**) Whole-mount ISH showing *Gata4* down-regulation in the heart of COET; $Mesp1^{Cre/+}$ mutant embryos (C and D) compared with wt (A and B) littermates at E8.5 and E9.5. Arrows indicate the inflow region of the heart.

of the putative TBEs that we have identified resides in a skeletal muscle-specific control region (36) upstream of *Mef2c* (Supplementary Material, Fig. S4A).

We also found a putative TBE in a conserved SHF-specific enhancer (Supplementary Material, Fig. S4B), previously described by Dodou *et al.* (35).

Chromatin immunoprecipitation (ChIP) experiments on C2C12 cells revealed that endogenous Tbx1 occupies both these sites (Fig. 8), suggesting that it may have a direct role in *Mef2c* transcriptional regulation.

Next, we carried out luciferase assays using a reporter construct carrying the SHF enhancer (SHF-Enh-Luc; Fig. 9A) to test its response to Tbx1 in C2C12 cells. The enhancer responded to transfected *Isl1* and *Gata4* but not to transfected *Tbx1* alone (Fig. 9B). In addition, as shown in the experiment with the *des*MEF2 reporter, Tbx1 did not inhibit Isl1-induced activation, but did interfere with Gata4-induced activation (Fig. 9C and D). The mutation of the TBE site resulted in a significant reduction in the response to Gata4 and in a milder, but still significant response to Tbx1 co-transfection (Fig. 9D). Thus, in this assay, the TBE is not completely required for Tbx1 to carry out its negative effect upon Gata4 activation, although this effect appears to be milder.

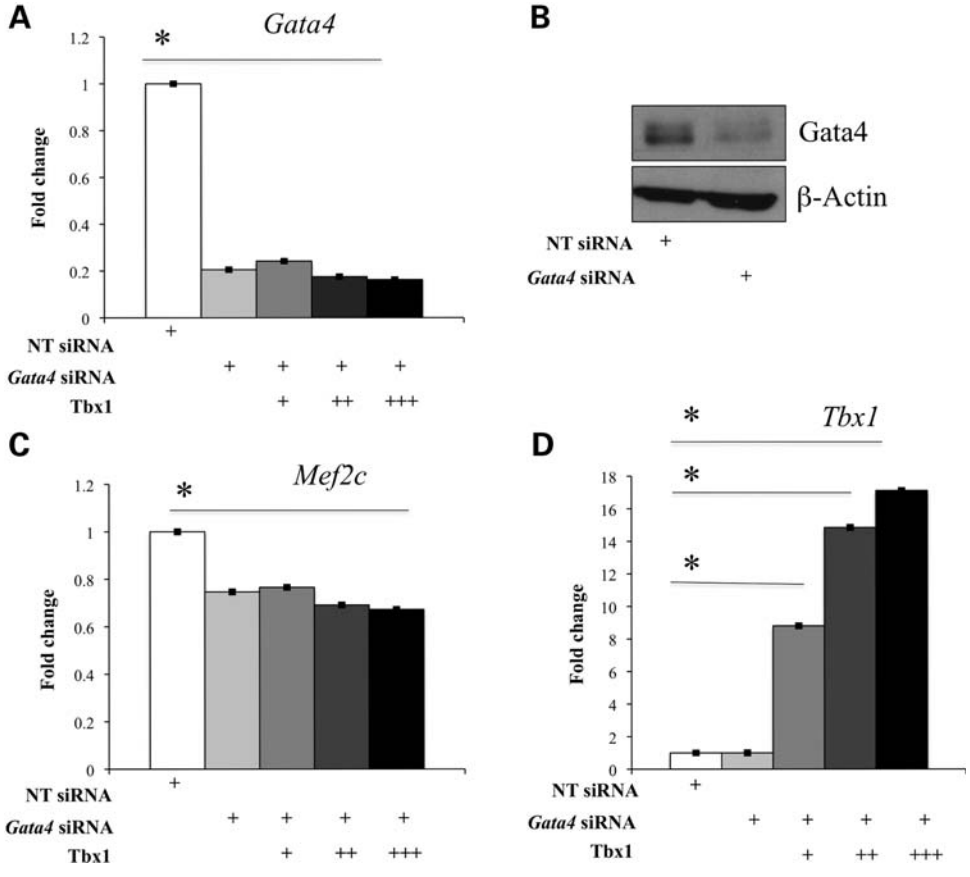

Figure 7. *Gata4* is required for *Mef2c* repression by *Tbx1* in C2C12 myoblasts. (**A** and **B**) siRNA-mediated knockdown of *Gata4* results in a reduction in mRNA and protein levels to ~20% of the wt level, as confirmed by qRT–PCR (A) and WB analysis (B). (**C** and **D**) qRT–PCR showed that *Gata4* knockdown and Tbx1 over-expression result, independently, in *Mef2c* down-regulation (C and D and Fig. 4A and B). In the absence of *Gata4*, over-expression of *Tbx1* does not result in further reduction in *Mef2c* expression (C). Values are means ± SE, $n = 3$, $^*P < 0.05$.

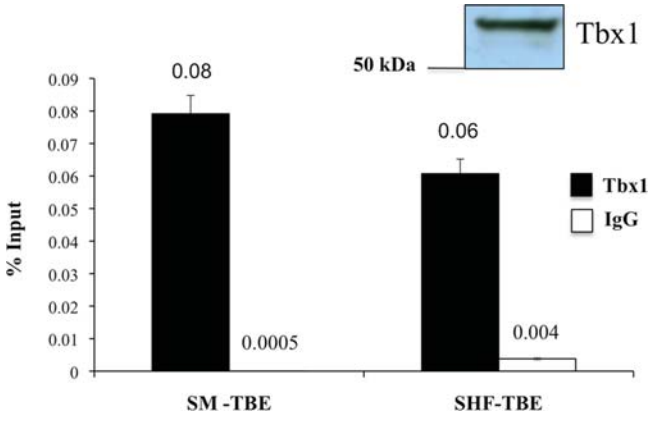

Figure 8. Endogenous Tbx1 binds conserved regulatory regions in the *Mef2c* locus. Small panel top-right: WB analysis of C2C12 nuclear extracts using an anti-Tbx1 antibody demonstrating endogenous expression of the protein. Graph: chromatin immunoprecipitation analysis of the *Mef2c* skeletal muscle and SHF TBEs performed in C2C12 myoblasts using an antibody against Tbx1 together with rabbit IgG as the background control. qRT–PCR analysis of an immunoprecipitated material was performed and percent of input for each sample is reported in the graph. Values are means ± SD, $n = 3$.

DISCUSSION

Dosage of *Tbx1* correlates well (though often not linearly) to phenotypic severity *in vivo* (9). With this work, we initiated an effort to correlate phenotypic changes with genome-wide transcriptional analysis, in order to identify candidate effectors that may be closely correlated with different phenotypic features. The experimental approach used here has some limitations, e.g. the whole embryo RNA analysis might smooth out or even hide tissue-specific changes of expression. In addition, stage-specific differences cannot be detected by our single-stage analysis. Nevertheless, our study was sufficient to identify a relatively subtle expression modulation of the *Mef2c* gene, which encodes a transcription factor critical in cardiac differentiation. *In vivo* and *in vitro* gain- and loss-of-function studies confirmed the negative correlation between *Tbx1* and *Mef2c* expression. This finding is consistent with the previously determined ability of Tbx1 to inhibit cardiomyocyte differentiation *in vivo* and *in vitro* (14). Our study also indicates that *Tbx1* over-expression has inhibitory effects upon *Mef2c* expression during skeletal muscle differentiation.

We asked how Tbx1 down-regulates *Mef2c* expression. Our data suggest three, non-mutually exclusive, mechanisms (Fig. 10). One is direct interaction with the *Mef2c* gene

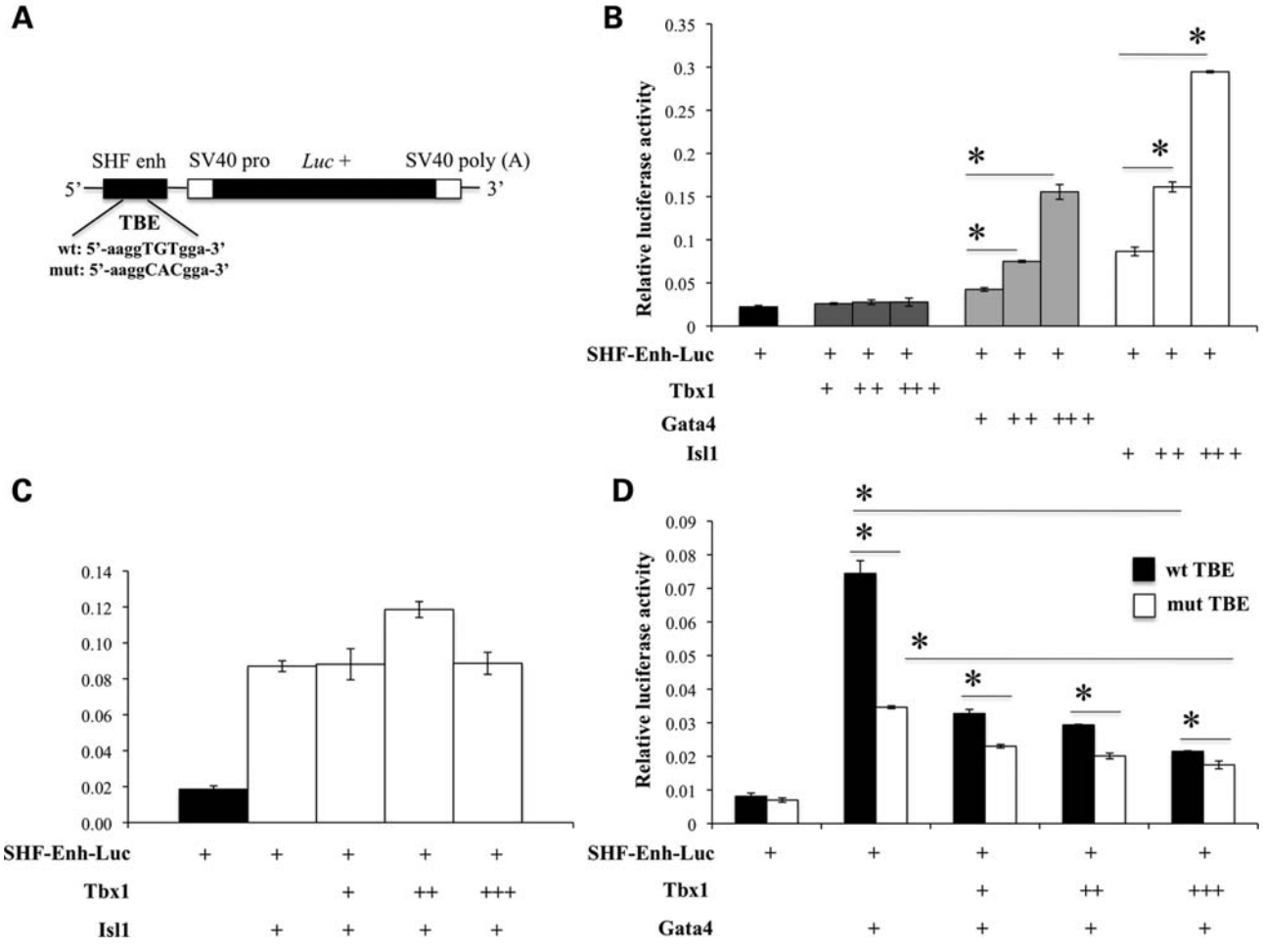

Figure 9. Response of the *Mef2c* SHF enhancer to Tbx1 expression in luciferase assays. (**A**) Scheme of the *Mef2c* SHF enhancer–luciferase construct. The sequence of the mutant TBE is indicated. (**B**) The enhancer responds well to graded amounts of transfected Isl1 and Gata4 but not to Tbx1. (**C**) Tbx1 does not significantly affect Isl1-induced activation of the enhancer. (**D**) Luciferase assay using a wt (black bars) or mutated (white bars) SHF enhancer. In both cases, Tbx1 can reduce Gata4-induced activation of the enhancer. However, the mutant SHF responds less well to Gata4, and Tbx1 inhibition is less obvious. Luciferase activity was normalized to β-galactosidase activity. Values are means ± SE, $n = 3$, $^{*}P < 0.05$.

(Fig. 10), as suggested by occupation of two TBE sites by Tbx1. The consequences of this interaction remain to be investigated, but they may be chromatin changes leading to transcriptional down-regulation. Our luciferase assay with a mutated TBE in the SHF resulted in very limited reduction in the capacity of Tbx1 to inhibit enhancer activity. However, because enhancer constructs are not properly chromatinized and are out of the normal context of the endogenous gene, it is difficult to draw conclusions from these data.

The second mechanism is mediated by a repressive effect of Tbx1 upon *Gata4* gene expression (Fig. 10), as seen *in vivo* (13) (data presented here). This mechanism is supported by tissue culture data, showing that silencing *Gata4* suppresses the ability of Tbx1 to down-regulate *Mef2c* in C2C12 cells. This effect would have negative consequences upon the expression of *Mef2c* because this gene is a target of Gata4. However, our *des*MEF2 reporter data indicate that Tbx1 is able to inhibit reporter activation in the presence of transfected *Gata4*, and in this scenario, the transcriptional regulation of the *Gata4* gene is irrelevant. It is more likely that Tbx1 interferes negatively upon the ability of the Gata4 protein to regulate *Mef2c* (Fig. 10). The third mechanism is also compatible with the results obtained by *Gata4* knockdown (Fig. 7). Tbx20 synergizes with Gata4 (and Isl1) to activate both the *Mef2c* and *Nkx2.5* SHF enhancers (37); Tbx1 may compete with another T-box protein and inhibit this synergy. Interestingly, in our luciferase assay with the SHF enhancer, the mutation of the TBE site significantly reduced the ability of Gata4 to activate the enhancer. This might be because of an endogenous T-box protein that synergizes with Gata4 in C2C12 cells. However, this is not Tbx20, as the gene encoding it is not expressed in these cells (our unpublished data). In addition, Gata4 and Tbx5 co-immunoprecipitate and cooperatively transactivate a luciferase atrial natriuretic factor reporter (38). However, Tbx1 does not co-immunoprecipitate with Gata4 in C2C12 cells (data not shown). Of note, co-transfection experiments showed the ability of Nkx2-5 and GATA4 to transactivate the minimal *Cx40* promoter, while Tbx5 repressed Nkx2-5/GATA4-mediated activation (39), demonstrating that T-box transcription factors could activate or repress transcription, depending on the specific context.

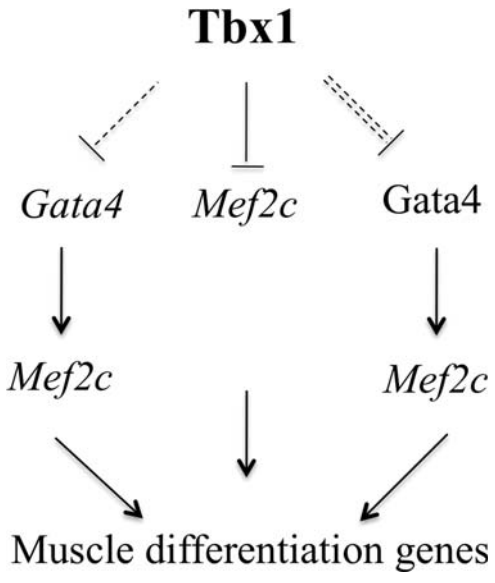

Figure 10. Schematic model of *Mef2c* regulation by Tbx1. Our data suggest three, non-mutually exclusive, mechanisms: (i) direct transcriptional regulation of *Mef2c* by Tbx1; (ii) negative regulation of *Gata4* expression and (iii) interference with Gata4-dependent activation of *Mef2c* (double-dashed line).

In summary, our results illustrate the power of multiallelic gene expression analysis as it identified a relatively subtle regulation of a gene encoding a developmentally critical transcription factor. The mechanisms by which Tbx1 regulates *Mef2c* expression appear to be complex and include direct interaction with the gene, regulation of *Gata4* expression, which in turn regulates *Mef2c*, and possibly interference with the Gata4 protein ability to regulate *Mef2c*.

The identification of the negative regulation of *Mef2c* by Tbx1 provides an additional clue as to how Tbx1 carries out its negative modulation of cardiomyocyte differentiation and provides a new link in the genetic network operating in cardiac progenitor cells.

MATERIALS AND METHODS

Mouse lines, breeding and genotyping

All the mouse mutant alleles used in this study have been previously reported: $Tbx1^{-}$ (7), $Tbx1^{Neo}$ (11), $Tbx1^{Neo2}$ (12), *COET* (10) and $Mesp1^{Cre}$ (40). The *COET* transgene (10) upon Cre-mediated recombination in average expresses a Tbx1 cDNA approximately twice as much as the level of one endogenous *Tbx1* allele (10).

Various homozygous and compound heterozygous mutants were generated by heterozygous mutant mating. Embryos were collected at E8.5 and E9.5, considering the day of observation of a vaginal plug to be E0.5. Mice were genotyped by PCR as described in the original reports.

Cell lines, plasmids and transfections

Mouse C2C12 myoblasts (ATCC) were cultured in Dulbecco's modified Eagle's medium (DMEM, Invitrogen) supplemented with 10% fetal bovine serum (Hyclone) at 37°C with 5% CO_2. To allow cells to differentiate, medium was changed to DMEM medium supplemented with 2% horse serum (Hyclone).

We have previously described the pCDNA-Tbx1-c-myc expression vector (11). The *des*MEF2-luc reporter construct (33) was kindly provided by Dr Eric N. Olson; the pCDNA3.1-Gata4-c-myc-His and pCDNA3.1-Ils1 were kindly provided by Dr Robert J. Schwartz.

The SHF-Enh-Luc reporter construct was generated by cloning the SHF minimal enhancer of the mouse *Mef2c* gene described by Dodou *et al*. (35) into the pGL3- Promoter Vector (Promega). The mutated SHF-Enh-Luc reporter construct was generated by substitution of three nucleotides in the conserved TBE of the original SHF-Enh-Luc reporter construct, using the QuikChange II Site- Directed Mutagenesis Kit (Stratagene) according to the manufacturer's instructions.

C2C12 cells were transiently transfected using the PolyFect Transfection Reagent (QIAGEN) according to the manufacturer's instructions; cells were collected 24 h after transfection for RNA or protein extraction.

For differentiation experiments, 24 h after transfection, medium was changed to differentiation medium and cells were collected at different days for RNA extraction.

Microarray-based gene expression analysis

Total RNA from E9.5 embryos with nine different genotypes ($Tbx1^{+/+}$, $Tbx1^{Neo2/+}$, $Tbx1^{Neo/+}$, $Tbx1^{+/-}$, $Tbx1^{Neo2/Neo2}$, $Tbx1^{Neo2/Neo}$, $Tbx1^{Neo2/-}$, $Tbx1^{Neo/Neo}$ and $Tbx1^{-/-}$) was isolated using TRIzol (Invitrogen) and cleaned using the RNeasy cleanup Kit (QIAGEN) according to the manufacturer's instructions. Procedures for cRNA preparation and GeneChip processing were performed at Boston University Microarray Resource Facility exactly as described in the Affymetrix GeneChip Expression Analysis Technical Manual (Affymetrix, Santa Clara, CA, USA, current version available at www.affymetrix.com). Briefly, total RNA integrity was verified using RNA 6000 Nano Assay RNA chips run in Agilent 2100 Bioanalyzer (Agilent Technologies). Total RNA was reverse transcribed using One Cycle cDNA Synthesis kit (Affymetrix) and the obtained double-stranded cDNA was purified with GeneChip Sample Cleanup Module (Affymetrix). cDNA was used as a template for *in vitro* transcription using GeneChip in vitro transcription (IVT) Labeling Kit (Affymetrix). The obtained biotin-labeled cRNA was purified using GeneChip Sample Cleanup Module (Affymetrix), fragmented and hybridized (10 μg) to the GeneChip Mouse 430 2.0 microarrays (Affymetrix) for 16 h in GeneChip Hybridization oven 640 at 45°C. For each genotype, we used two biological replicates, each hybridized to one array, with a total of 18 arrays. IVT and cRNA fragmentation quality controls were carried out by running an mRNA Nano assay in the Agilent 2100 Bioanalyzer. The hybridized samples were washed and stained using Affymetrix fluidics station 450 with streptavidin-R-phycoerythrin (SAPE) and the signal was amplified using a biotinylated goat anti-streptavidin antibody followed by another SAPE staining (Hybridization, Washing and Staining Kit, Affymetrix). Microarrays were immediately scanned using Affymetrix GeneArray Scanner 3000 7G Plus (Affymetrix). The data were analyzed with the

Bioconductor package 'Affy' using Robust Multiarray Average method for normalizing and summarizing probe level intensity measurements.

Statistical analysis of microarray data

We developed a strategy for statistical comparison of chip data aimed at identifying genes that responded to variations of *Tbx1* dosage. To discover which genes responded significantly, we computed the log ratio of all dosage points with respect to the control (wt) point for all genes. After this, we used a two-step filtering: in the first step, we made the assumption that if a gene is not responding to the dosage variation, then the area under the gene profile curve should be close to zero. We approximated this area by summing the square of the relative expression levels of all genes. Under the null hypothesis that a gene is not responding in the dosage series, this area should be close to zero, otherwise it should be higher. We approximated the area distribution with an exponential probability density function with the mean equal to the average of the area of all transcripts in the microarray. By using a *P*-value of 0.05, we selected a list of 2230 transcripts, including *Tbx1* (Supplementary Material, Table S1).

In the second step, we performed a more stringent test based on a Bayesian analysis of signals (41). This fully Bayesian approach allowed us to automatically identify and rank 497 differentially significant genes, whose expression is sensitive to *Tbx1* dosage (Supplementary Material, Table S2).

GO and cluster analyses

GO analysis (http://david.abcc.ncifcrf.gov/) was performed to identify specific biological pathways enriched in the list of 498 differentially expressed genes. The most significant terms included regulation of metabolic processes and regulation of gene expression (false discovery rate < 0.05).

Hierarchical clustering was performed on the list of 498 differentially expressed genes using the MATLAB software (http://www.mathworks.it/help/toolbox/stats/bq_679x-3.html#bq_6_ia). Four main clusters were identified and, for each cluster, we calculated the average profile and the associated standard deviation (SD).

TBE search

Upstream and intronic genomic sequences for human and mouse *Mef2c* were obtained from both the Ensembl and UCSC Genome Browser web sites and were aligned using the multisequence local alignment tool MULAN (http://mulan.dcode.org/). No specific Tbx1-binding consensus sequence has been identified so far; however, Tbx1 can activate, *in vitro*, the *Fgf10* promoter, through a conserved Tbx5-binding site (11). Multi-TF (http://multitf.dcode.org) transcription factor-binding site analysis was performed to find evolutionary conserved Tbx5-binding elements, in the aligned sequences. With this approach, we uncovered several TBEs in the *Mef2c* locus.

Quantitative real-time PCR

Total RNA was extracted from whole E9.5 wt and mutant embryos using TRIzol (Invitrogen) and from C2C12 using the RNeasy Mini Kit (QIAGEN). One microgram of total RNA was reverse transcribed using SuperScript III (Invitrogen) according to the manufacturer's instructions, in a total volume of 20 μl; the resulting cDNA was diluted 1:10. qRT–PCR was performed using SYBR Green for the detection of fluorescence during amplification. Each amplification reaction contained 25 μl of Platinum SYBR Green qPCR SuperMix-UDG (Invitrogen), 0.2 μg each of forward and reverse primers and 1 μl of diluted cDNA. All primers were designed with annealing temperatures of 58–62°C. PCR conditions were: 50°C for 2 min, 95°C for 10 min, 40 cycles of 95°C for 15 s, 60°C for 1 min and followed by a dissociation stage of 95°C for 15 s and 60°C for 15 s. All the genes were amplified on a 7900 HT Fast Real-Time PCR System (Applied Biosystems). PCR amplifications were performed in triplicate and at least three separate analyses were carried out for each gene. Melting curve analysis was performed after each run to check for the presence of non-specific PCR products and primer dimers. The qRT–PCR results, recorded as threshold cycle numbers (C_t) were normalized using GAPDH as an internal control and analyzed using the comparative C_t method ($2^{-\Delta\Delta C_t}$ method) (42,43).

In situ hybridization

Digoxigenin-labeled RNA probes were prepared by standard methods (Roche). *Mef2c* and *Gata4* probes were kindly provided by Dr Brian L. Black. Embryos were dissected in di-ethylpolycarbonate (Sigma Aldrich)-treated phosphate-buffered saline (PBS) and fixed overnight in 4% paraformaldehyde–PBS (Sigma Aldrich) at 4°C.

For ISH on cryosections, embryos were cryoprotected with increasing concentrations of sucrose (Sigma Aldrich), treated with a mixture of 1 part 30% sucrose and 1 part OCT for at least 2 h at 4°C, embedded in OCT and cut to generate 10–12 μm sections. After post-fixation in 4% paraformaldehyde–PBS, sections were incubated in triethanolamine buffer (0.2% acetic acid and 1% triethanolamine, Sigma Aldrich) containing acetic anhydride and washed twice in PBS for 5 min. The sections were then prehybridized for 1 h at 70°C in the hybridization mixture (50% formamide from Sigma Aldrich, 5× saline-sodium citrate (SSC), salmon sperm DNA 40 μg/ml and 25 mg/ml yeast tRNA from Invitrogen). The probes were denatured for 5 min at 80°C and added to the hybridization mix (400 ng/ml). The hybridization reaction was carried out over night at 70°C; prehybridization and hybridization were performed in a box saturated with a 5× SSC–50% formamide solution to avoid evaporation. After incubation, the sections were washed twice with MABT (50 mM maleic acid, pH 7.5, 250 mM NaCl and 0.1% Tween-20, Sigma Aldrich), treated with MABT containing 10% sheep serum for 1 h at room temperature and then incubated with alkaline phosphatase-coupled anti-digoxigenin antibody (Roche) diluted 1:2000 in MABT containing 10% sheep serum, overnight at 4°C. The day after, sections were washed with MABT and equilibrated for 5 min in Buffer 3 (Tris–HCl

100 mM, NaCl 100 mM and $MgCl_2$ 50 mM, pH 9.5); color development was performed at room temperature (time depending on the amount of transcripts to be detected) in Buffer 3 containing nitro blue tetrazolium and 5-bromo-4-chloro-3-indolyl phosphate (Roche). Staining was stopped by a wash in PBS containing 0.1% Tween-20; sections were rehydrated for 5 min in deionized water and then dehydrated through successive baths of EtOH (70, 95 and 100%) and xylol, and mounted in Eukitt resin (O. Kindler GmbH & Co.).

Whole-mount ISH was performed according to the previously published methods (44). At least three somite staged wt and mutant embryos were analyzed with each probe.

Western blotting

Nuclear proteins were extracted as described previously (18). The following primary antibodies were used: rabbit anti-Tbx1 (Abcam, 1:1000), goat anti-Mef2c (Santa Cruz Biotechnology, 1:1000), rabbit anti-Gata4 (Santa Cruz Biotechnology, 1:1000), monoclonal anti-c-myc (Sigma-Aldrich 1:1000) and monoclonal anti-β-Actin (Sigma-Aldrich 1:10 000). The following secondary antibodies were used: horseradish peroxidase-conjugated (HRP) anti-rabbit and anti-mouse (GE Healthcare, 1:10 000) and HRP-conjugated anti-goat (Santa Cruz Biotechnology, 1:5000). The HRP-derived signal was detected using the Amersham ECL and ECL Plus Western Blotting Detection Reagents (GE Healthcare).

Luciferase assay

For luciferase assays, mouse C2C12 myoblasts were plated in 24-wells and transfected with PolyFect Transfection Reagent (QIAGEN) according to the manufacturer's instructions. The *des*MEF2-luc reporter construct and, for single experiments, the pCDNA-Tbx1-c-myc, pCDNA3.1-Gata4-c-myc-His and pCDNA3.1-Ils1 plasmids were always co-transfected with a pCMV-β-Gal expression vector (Clontech); at 24 h after transfection, cell extracts were prepared and activities of β-galactosidase and *Firefly* luciferase were measured using the Luciferase Assay System (Promega) and the Beta-Glo Assay System (Promega), respectively, on a GLOMAX 96 microplate luminometer (Promega). Relative luciferase activity (*Firefly* luciferase for reporter and β-galactosidase for normalization of transfection efficiency) was measured following manufacturer's instructions (Promega). The data represent the means and SDs of at least three independent transfections.

RNA interference

Gata4 interference in C2C12 myoblasts was achieved by using a set of four different siRNAs specifically directed against the mouse *Gata4* locus (ON-TARGET plus SMART Pool, Thermo Scientific). As negative control, we used a pool of siRNAs that virtually targeted no mouse genes (ON-TARGET plus Negative Control, Thermo Scientific). Cells were plated in six wells and transfected with 50 nM/well of siRNAs using Lipofectamine 2000 (Invitrogen) according to the manufacturer's instructions. The *Gata4* mRNA level was measured by qRT–PCR and the Gata4 protein level by WB as described above.

ChIP assay

ChIP assay was performed as described previously (45). Sonication was performed for 10 cycles of 15 s on and 60 s off using a Soniprep 150 (Measuring and Scientific Equipment). Immunoprecipitation was performed overnight at 4°C with an antibody against Tbx1 (Abcam, 4/100 μg of chromatin); normal rabbit immunoglobulin G (IgG) was used as the background control.

Results were quantified by qRT–PCR using the primers listed in Supplementary Material, Table S3, and the enrichment of DNA was calculated in terms of percent of input, as described previously (46). PCR amplifications were performed in triplicate from three independent experiments.

Statistical analysis

All data were expressed as means ± standard error or SD from three independent experiments. Differences between groups were examined for statistical analysis using a two-tailed Student's *t*-test. Values of $P < 0.05$ were considered significant.

SUPPLEMENTARY MATERIAL

Supplementary Material is available at *HMG* online.

ACKNOWLEDGEMENTS

We thank Dr Eric N. Olson and Dr Robert J. Schwartz for reagents. We thank Wei Wen for technical assistance with *in situ* hybridization experiments, the Core Facilities of the Institute of Genetics and Biophysics (Integrated Microscopy and Mouse Transgenic) for support and the Boston University Microarray Resource Facility.

Conflict of Interest statement. None declared.

FUNDING

This work was supported by the European Union (FP7 CardioGeNet project), the Italian Telethon Foundation (grant GGP11029) and the Italian Ministry of Research and Education (PRIN 2009J7F5WA 002 to A.B.). Funding to pay the Open Access publication charges for this article was provided by the Italian Telethon Foundation.

REFERENCES

1. Yagi, H., Furutani, Y., Hamada, H., Sasaki, T., Asakawa, S., Minoshima, S., Ichida, F., Joo, K., Kimura, M., Imamura, S. *et al.* (2003) Role of TBX1 in human del22q11.2 syndrome. *Lancet*, **362**, 1366–1373.
2. Stoller, J.Z. and Epstein, J.A. (2005) Identification of a novel nuclear localization signal in Tbx1 that is deleted in DiGeorge syndrome patients harboring the 1223delC mutation. *Hum. Mol. Genet.*, **14**, 885–892.
3. Paylor, R., Glaser, B., Mupo, A., Ataliotis, P., Spencer, C., Sobotka, A., Sparks, C., Choi, C.H., Oghalai, J., Curran, S. *et al.* (2006) Tbx1 haploinsufficiency is linked to behavioral disorders in mice and humans: implications for 22q11 deletion syndrome. *Proc. Natl Acad. Sci. USA*, **103**, 7729–7734.
4. Torres-Juan, L., Rosell, J., Morla, M., Vidal-Pou, C., Garcia-Algas, F., de la Fuente, M.A., Juan, M., Tubau, A., Bachiller, D., Bernues, M. *et al.* (2007) Mutations in TBX1 genocopy the 22q11.2 deletion and duplication

syndromes: a new susceptibility factor for mental retardation. *Eur. J. Hum. Genet.*, **15**, 658–663.
5. Zweier, C., Sticht, H., Aydin-Yaylagul, I., Campbell, C.E. and Rauch, A. (2007) Human TBX1 missense mutations cause gain of function resulting in the same phenotype as 22q11.2 deletions. *Am. J. Hum. Genet.*, **80**, 510–517.
6. Jerome, L.A. and Papaioannou, V.E. (2001) DiGeorge syndrome phenotype in mice mutant for the T-box gene, Tbx1. *Nat. Genet.*, **27**, 286–291.
7. Lindsay, E.A., Vitelli, F., Su, H., Morishima, M., Huynh, T., Pramparo, T., Jurecic, V., Ogunrinu, G., Sutherland, H.F., Scambler, P.J. *et al.* (2001) Tbx1 haploinsufficiency in the DiGeorge syndrome region causes aortic arch defects in mice. *Nature*, **410**, 97–101.
8. Merscher, S., Funke, B., Epstein, J.A., Heyer, J., Puech, A., Lu, M.M., Xavier, R.J., Demay, M.B., Russell, R.G. and Factor, S. (2001) TBX1 is responsible for cardiovascular defects in velo-cardio-facial/DiGeorge syndrome. *Cell*, **104**, 619–629.
9. Zhang, Z. and Baldini, A. (2008) In vivo response to high-resolution variation of Tbx1 mRNA dosage. *Hum. Mol. Genet.*, **17**, 150–157.
10. Vitelli, F., Huynh, T. and Baldini, A. (2009) Gain of function of Tbx1 affects pharyngeal and heart development in the mouse. *Genesis*, **47**, 188–195.
11. Xu, H., Morishima, M., Wylie, J.N., Schwartz, R.J., Bruneau, B.G., Lindsay, E.A. and Baldini, A. (2004) Tbx1 has a dual role in the morphogenesis of the cardiac outflow tract. *Development*, **131**, 3217–3227.
12. Zhang, Z., Huynh, T. and Baldini, A. (2006) Mesodermal expression of Tbx1 is necessary and sufficient for pharyngeal arch and cardiac outflow tract development. *Development*, **133**, 3587–3595.
13. Liao, J., Aggarwal, V.S., Nowotschin, S., Bondarev, A., Lipner, S. and Morrow, B.E. (2008) Identification of downstream genetic pathways of Tbx1 in the second heart field. *Dev. Biol.*, **316**, 524–537.
14. Chen, L., Fulcoli, F.G., Tang, S. and Baldini, A. (2009) Tbx1 regulates proliferation and differentiation of multipotent heart progenitors. *Circ. Res.*, **105**, 842–851.
15. Vitelli, F., Taddei, I., Morishima, M., Meyers, E.N., Lindsay, E.A. and Baldini, A. (2002) A genetic link between Tbx1 and fibroblast growth factor signaling. *Development*, **129**, 4605–4611.
16. Hu, T., Yamagishi, H., Maeda, J., McAnally, J., Yamagishi, C. and Srivastava, D. (2004) Tbx1 regulates fibroblast growth factors in the anterior heart field through a reinforcing autoregulatory loop involving forkhead transcription factors. *Development*, **131**, 5491–5502.
17. Chen, L., Mupo, A., Huynh, T., Cioffi, S., Woods, M., Jin, C., McKeehan, W., Thompson-Snipes, L., Baldini, A. and Illingworth, E.A. (2010) Tbx1 regulates Vegfr3 and is required for lymphatic vessel development. *J. Cell Biol.*, **189**, 417–424.
18. Fulcoli, F.G., Huynh, T., Scambler, P.J. and Baldini, A. (2009) Tbx1 regulates the BMP-Smad1 pathway in a transcription independent manner. *PLoS One*, **4**, e6049.
19. Massague, J., Seoane, J. and Wotton, D. (2005) Smad transcription factors. *Genes Dev.*, **19**, 2783–2810.
20. Chen, C.Y. and Schwartz, R.J. (1996) Recruitment of the tinman homolog Nkx-2.5 by serum response factor activates cardiac alpha-actin gene transcription. *Mol. Cell. Biol.*, **16**, 6372–6384.
21. Liu, N. and Olson, E.N. (2006) Coactivator control of cardiovascular growth and remodeling. *Curr. Opin. Cell Biol.*, **18**, 715–722.
22. Pollock, R. and Treisman, R. (1991) Human SRF-related proteins: DNA-binding properties and potential regulatory targets. *Genes Dev.*, **5**, 2327–2341.
23. Leifer, D., Krainc, D., Yu, Y.T., McDermott, J., Breitbart, R.E., Heng, J., Neve, R.L., Kosofsky, B., Nadal-Ginard, B. and Lipton, S.A. (1993) MEF2C, a MADS/MEF2-family transcription factor expressed in a laminar distribution in cerebral cortex. *Proc. Natl Acad. Sci. USA*, **90**, 1546–1550.
24. Edmondson, D.G., Lyons, G.E., Martin, J.F. and Olson, E.N. (1994) Mef2 gene expression marks the cardiac and skeletal muscle lineages during mouse embryogenesis. *Development*, **120**, 1251–1263.
25. Lyons, G.E., Micales, B.K., Schwarz, J., Martin, J.F. and Olson, E.N. (1995) Expression of mef2 genes in the mouse central nervous system suggests a role in neuronal maturation. *J. Neurosci.*, **15**, 5727–5738.
26. Lin, Q., Lu, J., Yanagisawa, H., Webb, R., Lyons, G.E., Richardson, J.A. and Olson, E.N. (1998) Requirement of the MADS-box transcription factor MEF2C for vascular development. *Development*, **125**, 4565–4574.
27. Bi, W., Drake, C.J. and Schwarz, J.J. (1999) The transcription factor MEF2C-null mouse exhibits complex vascular malformations and reduced cardiac expression of angiopoietin 1 and VEGF. *Dev. Biol.*, **211**, 255–267.
28. Lin, Q., Schwarz, J., Bucana, C. and Olson, E.N. (1997) Control of mouse cardiac morphogenesis and myogenesis by transcription factor MEF2C. *Science*, **276**, 1404–1407.
29. Monks, D.C. and Morrow, B.E. (2012) Identification of putative retinoic acid target genes downstream of mesenchymal Tbx1 during inner ear development. *Dev. Dyn.*, **241**, 563–573.
30. Huang da, W., Sherman, B.T. and Lempicki, R.A. (2009) Systematic and integrative analysis of large gene lists using DAVID bioinformatics resources. *Nat. Protoc.*, **4**, 44–57.
31. Huang da, W., Sherman, B.T. and Lempicki, R.A. (2009) Bioinformatics enrichment tools: paths toward the comprehensive functional analysis of large gene lists. *Nucleic Acids Res.*, **37**, 1–13.
32. Andres, V. and Walsh, K. (1996) Myogenin expression, cell cycle withdrawal, and phenotypic differentiation are temporally separable events that precede cell fusion upon myogenesis. *J. Cell Biol.*, **132**, 657–666.
33. Naya, F.J., Wu, C., Richardson, J.A., Overbeek, P. and Olson, E.N. (1999) Transcriptional activity of MEF2 during mouse embryogenesis monitored with a MEF2-dependent transgene. *Development*, **126**, 2045–2052.
34. Wu, H., Naya, F.J., McKinsey, T.A., Mercer, B., Shelton, J.M., Chin, E.R., Simard, A.R., Michel, R.N., Bassel-Duby, R., Olson, E.N. and Williams, R.S. (2000) MEF2 responds to multiple calcium-regulated signals in the control of skeletal muscle fiber type. *EMBO J.*, **19**, 1963–1973.
35. Dodou, E., Verzi, M.P., Anderson, J.P., Xu, S.M. and Black, B.L. (2004) Mef2c is a direct transcriptional target of ISL1 and GATA factors in the anterior heart field during mouse embryonic development. *Development*, **131**, 3931–3942.
36. Wang, D.Z., Valdez, M.R., McAnally, J., Richardson, J. and Olson, E.N. (2001) The Mef2c gene is a direct transcriptional target of myogenic bHLH and MEF2 proteins during skeletal muscle development. *Development*, **128**, 4623–4633.
37. Takeuchi, J.K., Mileikovskaia, M., Koshiba-Takeuchi, K., Heidt, A.B., Mori, A.D., Arruda, E.P., Gertsenstein, M., Georges, R., Davidson, L., Mo, R. *et al.* (2005) Tbx20 dose-dependently regulates transcription factor networks required for mouse heart and motoneuron development. *Development*, **132**, 2463–2474.
38. Garg, V., Kathiriya, I.S., Barnes, R., Schluterman, M.K., King, I.N., Butler, C.A., Rothrock, C.R., Eapen, R.S., Hirayama-Yamada, K., Joo, K. *et al.* (2003) GATA4 mutations cause human congenital heart defects and reveal an interaction with TBX5. *Nature*, **424**, 443–447.
39. Linhares, V.L., Almeida, N.A., Menezes, D.C., Elliott, D.A., Lai, D., Beyer, E.C., Campos de Carvalho, A.C. and Costa, M.W. (2004) Transcriptional regulation of the murine Connexin40 promoter by cardiac factors Nkx2-5, GATA4 and Tbx5. *Cardiovasc. Res.*, **64**, 402–411.
40. Saga, Y., Miyagawa-Tomita, S., Takagi, A., Kitajima, S., Miyazaki, J. and Inoue, T. (1999) MesP1 is expressed in the heart precursor cells and required for the formation of a single heart tube. *Development*, **126**, 3437–3447.
41. Angelini, C., Cutillo, L., De Canditiis, D., Mutarelli, M. and Pensky, M. (2008) BATS: a Bayesian user-friendly software for analyzing time series microarray experiments. *BMC Bioinformatics*, **9**, 415; doi:10.1186/1471-2105-9-415.
42. Livak, K.J. and Schmittgen, T.D. (2001) Analysis of relative gene expression data using real-time quantitative PCR and the 2(−Delta Delta C(T)) method. *Methods*, **25**, 402–408.
43. Schmittgen, T.D. and Livak, K.J. (2008) Analyzing real-time PCR data by the comparative C(T) method. *Nat. Protoc.*, **3**, 1101–1108.
44. Wilkinson, D.G. (1992) Whole-mount *in situ* hybridization of vertebrate embryos. *In Situ Hybridization: A Practical Approach*. IRL Press, Oxford, UK, pp. 75–83.
45. Wu, Y., Zhang, X., Salmon, M., Lin, X. and Zehner, Z.E. (2007) TGFbeta1 regulation of vimentin gene expression during differentiation of the C2C12 skeletal myogenic cell line requires Smads, AP-1 and Sp1 family members. *Biochim. Biophys. Acta*, **1773**, 427–439.
46. Chakrabarti, S.K., James, J.C. and Mirmira, R.G. (2002) Quantitative assessment of gene targeting *in vitro* and *in vivo* by the pancreatic transcription factor, Pdx1. Importance of chromatin structure in directing promoter binding. *J. Biol. Chem.*, **277**, 13286–13293.